CHEMISTRY & SUSTAINABILITY

CHEMSUSCHEM

ENERGY & MATERIALS

Accepted Article

Title: Highly Active Alkaline Earth Metals and Lanthanum-Doped NaTaO3 Photocatalysts for CO2 Reduction to Form CO Using Water as an Electron Donor

Authors: Haruka Nakanishi, Kosuke Iizuka, Tomoaki Takayama, Akihide Iwase, and Akihiko Kudo

To be cited as: *ChemSusChem* 10.1002/cssc.201601360

Link to VoR: http://dx.doi.org/10.1002/cssc.201601360

A Journal of

ChemPubSoc Europe

WILEY-VCH

www.chemsuschem.org

Highly Active Alkaline Earth Metals and Lanthanum-Doped $NaTaO_3$ Photocatalysts for CO_2 Reduction to Form CO Using Water as an Electron Donor

Haruka Nakanishi,[a] Kosuke Iizuka,[a] Tomoaki Takayama,[a] Akihide Iwase,[a, b] Akihiko Kudo*[a, b]

Abstract: Mg, Ca, Sr, Ba and La-doped $NaTaO_3$ has arisen as highly active photocatalysts for CO_2 reduction to form CO using water as an electron donor accompanied by O_2 evolution under UV irradiation and bubbling of 1 atmosphere of CO_2 when an Ag cocatalyst was loaded on those photocatalysts. CO, H_2 and O_2 simultaneously formed. The ratio of the number of reacted electrons to that of holes was almost unity. This result indicated that water was consumed as an electron donor. A liquid-phase reduction method for loading of the Ag cocatalyst was superior to photodeposition and impregnation methods. Ag cocatalyst-loaded $NaTaO_3$:Ba was the most active photocatalyst in water with no additives. Addition of bases such as hydrogencarbonate was effective to enhance the CO formation for Mg, Ca, Sr, Ba and La-doped $NaTaO_3$ photocatalysts with an Ag cocatalyst. Ca and Sr-doped $NaTaO_3$ photocatalysts especially showed high activity as well as the Ba-doped photocatalyst in the aqueous $NaHCO_3$ solution. The selectivity for the CO formation ($CO/(CO+H_2)$) on Ca, Sr and Ba-doped $NaTaO_3$ photocatalysts with Ag cocatalyst reached around 90%.

Introduction

Photocatalytic reduction of CO_2 has attracted attention from a viewpoint of artificial photosynthesis. A TiO_2 photocatalyst has mainly been studied so far.[1–5] It has been reported that the TiO_2 photocatalyst produces formic acid, methanol and methane without cocatalysts, and formic acid, formaldehyde, methane and other reduction products with cocatalysts. Sayama and coworkers have reported a ZrO_2 photocatalyst with 5.0 eV of a band gap for water splitting and CO_2 reduction accompanied by O_2 evolution.[6–7] The ZrO_2 photocatalyst possesses a high conduction band level resulting in showing the activity for the CO_2 reduction without any cocatalysts. The selectivity for CO formation is improved by loading a Cu cocatalyst.[7] They have also found the positive effect of addition of Na_2CO_3 and $NaHCO_3$ on water splitting and CO_2 reduction. However, 12% of the selectivity for the CO formation is not satisfying. We have also reported a $BaLa_4Ti_4O_{15}$ photocatalyst with 3.9 eV of a band gap for water splitting and CO_2 reduction.[8–10] The $BaLa_4Ti_4O_{15}$ photocatalyst shows relatively high activity for water splitting when a NiO_x cocatalyst is loaded. Moreover, an Ag cocatalyst-loaded $BaLa_4Ti_4O_{15}$ photocatalyst is active for CO_2 reduction to form CO using water as an electron donor. Although the selectivity for the CO formation is much higher than that over a Cu cocatalyst-loaded ZrO_2 photocatalyst, it still remains 69%. In this case, the Ag cocatalyst plays an important role for the photocatalytic CO_2 reduction. Similarly, $KCaSrTa_5O_{15}$, $ZnTa_2O_6$, SrO-modified Ta_2O_5, Zn-doped Ga_2O_3, $ZnGa_2O_4$, $La_2Ti_2O_7$ and $CaTiO_3$ photocatalysts also show activity for CO_2 reduction to form CO by loading the Ag cocatalyst.[11–18] These metal oxide photocatalysts respond to only UV light because of their wide band gaps. Recently, we have successfully demonstrated CO_2 reduction to form CO accompanied by certain O_2 generation due to water oxidation under visible light irradiation using a powdered Z-scheme system consisting of $CuGaS_2$ as a CO_2-reducing photocatalyst, $CoO_x/BiVO_4$ as an O_2-evolving photocatalyst and reduced graphene oxide (RGO) as a solid-state electron mediator.[19] However, the number of the photocatalysts for CO_2 reduction is limited even under UV irradiation at the present stage. Exploration of highly efficient photocatalysts for CO_2 reduction is still an important research topic.

Mg, Ca, Sr, Ba and La-doped $NaTaO_3$ ($NaTaO_3$:A (A = Mg, Ca, Sr, Ba and La)) photocatalysts with 4.1 eV of a band gap show high activities for water splitting.[20–23] Their conduction bands formed by Ta5d orbitals are thermodynamically preferable for the CO_2 reduction. Therefore, it is expected that the $NaTaO_3$:A (A = Mg, Ca, Sr, Ba and La) photocatalysts show high activity for the CO_2 reduction using water as an electron donor. Recently, several groups have reported CO_2 reduction on $NaTaO_3$ photocatalysts in an aqueous solution.[24–26] Small amounts of hydrocarbons and alcohols are obtained. However, O_2 evolution is not observed despite the absence of sacrificial electron donor, indicating that the ratio of the number of reacted electrons to that of holes is not unity.

In the present study, effects of an Ag cocatalyst on photocatalytic CO_2 reduction over $NaTaO_3$:A (A = Mg, Ca, Sr, Ba and La) were examined. The effects of acid and base on the photocatalytic CO_2 reduction were also investigated to improve the activity and to clarify the reactant species, CO_3^{2-}, HCO_3^- or a CO_2 molecule.

[a] Ms. H. Nakanishi, Mr. K. Iizuka, Dr. T. Takayama, Prof. A. Iwase, Prof. A. Kudo
Department of Applied Chemistry, Faculty of Science, Tokyo University of Science, 1-3 Kagurazaka, Shinjuku-ku, Tokyo, 162-8601, Japan
E-mail: *a-kudo@rs.kagu.tus.ac.jp*
[b] Prof. A. Iwase, Prof. A. Kudo
Photocatalysis International Research Center, Research Institute for Science and Technology, Tokyo University of Science, 2641 Yamazaki, Noda-shi, Chiba, 278-8510, Japan

Supporting information for this article is given via a link at the end of the document.

Results and Discussion

Photocatalytic reduction of CO_2

Table 1 shows a loading effect of cocatalysts on photocatalytic CO_2 reduction over $NaTaO_3$:A (A = Mg, Ca, Sr, Ba and La). We have reported that these photocatalysts were active for water splitting without cocatalysts.[20−23] Only water splitting proceeded on the pristine $NaTaO_3$:A (A = Mg, Ca, Sr, Ba and La) photocatalysts even under CO_2 bubbling of 1 atm (Entries 1−6), indicating that they were not active for CO_2 reduction without cocatalysts. In contrast, all of Ag-loaded photocatalysts showed activities for CO_2 reduction to form CO (Entries 7−13). Formic acid and methane were not detected. Ba was the most effective dopant among alkaline earth metals and lanthanum under the experimental condition in Table 1. A liquid-phase reduction method for loading of the Ag cocatalyst was superior to photodeposition and impregnation methods for the CO formation on the Ag/$NaTaO_3$:Ba photocatalyst (Entries 12, 14−16) as seen for Ag/$BaLa_4Ti_4O_{15}$.[9] The rate of CO formation was similar to that of H_2 formation when 1 wt% of the Ag cocatalyst was loaded on the $NaTaO_3$:Ba photocatalyst by the liquid-phase reduction method (Entry 16). The activities for CO_2 reduction using other cocatalysts were negligible (Entries 17−23). NiO, Ru and Au cocatalysts that are good cocatalysts for water splitting[9, 10, 27] just enhanced water splitting even under a CO_2 atmosphere (Entries 17, 20 and 23). Cu was also an effective cocatalyst for water splitting under the present experimental condition (Entry 19).

Table 1. CO_2 reduction over $NaTaO_3$:A (A = Mg, Ca, Sr, Ba and La) photocatalysts with various cocatalysts.[a]

Entry	Dopant	Cocatalyst (wt%)	Loading method	Activity / μmol h^{-1}			CO selectivity
				H_2	O_2	CO	%
1	None	None	−	152	76	0	0
2	Mg(5%)	None	−	49	23	trace	−
3	Ca(5%)	None	−	74	36	0	0
4	Sr(5%)	None	−	181	66	0	0
5	Ba(5%)	None	−	182	79	trace	−
6	La(2%)	None	−	230	109	trace	−
7	None	Ag(1.0)	Photodeposition	32	16	1.4	4
8	Mg(5%)	Ag(0.5)	Photodeposition	32	15	1.8	5
9	Ca(5%)	Ag(1.0)	Photodeposition	57	28	4.2	7
10	Sr(5%)	Ag(1.0)	Photodeposition	47	24	3.9	8
11	Ba(5%)	Ag(0.5)	Photodeposition	96	43	1.7	2
12	Ba(5%)	Ag(1.0)	Photodeposition	65	30	7.4	10
13	La(2%)	Ag(1.0)	Photodeposition	103	46	1	1
14	Ba(5%)	Ag(1.0)	Impregnation[b]	68	33	0.6	1
15	Ba(5%)	Ag(1.0)	Impregnation[b]+H_2 red[c]	39	18	1.4	3
16	Ba(5%)	Ag(1.0)	Liquid-phase reduction	20	20	25	56
17	Ba(5%)	NiO(0.2)	Impregnation[b]	2778	1314	trace	−
18	Ba(5%)	Ni(0.5)	Photodeposition	234	110	trace	−
19	Ba(5%)	Cu(0.5)	Photodeposition	218	100	trace	−
20	Ba(5%)	Ru(0.2)	Photodeposition	788	388	trace	−
21	Ba(5%)	Rh(0.5)	Photodeposition	31	13	trace	−
22	Ba(5%)	Pd(1.0)	Photodeposition	43	16	trace	−
23	Ba(5%)	Au(1.0)	Photodeposition	685	360	trace	−

[a] Catalyst: 0.25−0.5 g, reactant solution: water (360−370 mL), CO_2 flow rate: 30 mL min^{-1}, light source: a 400 W high-pressure mercury lamp, reactor: an inner irradiation quartz cell. [b] 723 K for 1 h, [c] 473 K for 2 h. CO selectivity (%) = (Rate of CO formation)/(Sum of rates of H_2 and CO formation)×100.

Effects of additions of acid and base on photocatalytic CO_2 reduction

Effects of additions of acid and base into a reactant solution on CO_2 reduction over Ag/$NaTaO_3$:A (A = Mg, Ca, Sr, Ba and La) photocatalysts are shown in Table 2. The effect of hydrogencarbonate on the photocatalytic CO_2 reduction was significant not only for the Ba-doped photocatalyst but also for Mg, Ca, Sr and La-doped photocatalysts (Entries 24−28). High activities were especially obtained when Ca, Sr and Ba dopants were employed.

The effects of acid and base on the photocatalytic activity were examined using Ag(3 wt%)/$NaTaO_3$:Ba in detail. The

Table 2. Effect of reactant solution on photocatalytic CO_2 reduction over $NaTaO_3$:A (A = Mg, Ca, Sr, Ba and La) with Ag cocatalyst loaded by a liquid-phase reduction method.[a]

Entry	Dopant	Ag cocatalyst / wt%	Additive (mol L^{-1})	pH[b]	Activity / μmol h^{-1}			CO selectivity %
					H_2	O_2	CO	
24	Mg(5%)	0.35	$NaHCO_3$ (0.1)	7.0	12	12	14	54
25	Ca(5%)	2.0	$NaHCO_3$ (0.1)	7.0	15	84	148	91
26	Sr(5%)	2.0	$NaHCO_3$ (0.1)	7.0	28	102	176	86
27	Ba(5%)	3.0	$NaHCO_3$ (0.1)	7.0	24	76	125	84
28	La(2%)	2.0[c]	$NaHCO_3$ (0.1)	7.0	80	59	50	38
29	Ba(5%)	3.0	None	4.3	41	43	44	52
30	Ba(5%)	3.0	Na_2CO_3 (0.05)	7.4	3	37	63	95
31	Ba(5%)	3.0	NaOH (0.1)	7.7	10	44	74	88
32	Ba(5%)	3.0	$KHCO_3$ (0.1)	7.0	10	51	84	89
33	Ba(5%)	3.0	K_2CO_3 (0.05)	7.5	9	33	45	83
34	Ba(5%)	3.0	KOH (0.1)	7.5	10	58	88	90
35	Ba(5%)	3.0	H_2SO_4	2.6	177	84	15	8
36	Ba(5%)	3.0	NaCl (0.1)	5.5	28	21	16	36
37	Ba(5%)	3.0	Na_2SO_4 (0.05)	5.0	35	37	42	55

[a] Photocatalyst: 0.25−0.5 g, reactant solution: water (360 mL), CO_2 flow late: 30 mL min^{-1}, light source: a 400 W high-pressure mercury lamp, reactor: an inner irradiation quartz cell. [b] After CO_2 bubbling, [c] photodeposition. CO selectivity (%) = (Rate of CO formation)/(Sum of rates of H_2 and CO formation)×100.

selectivity for CO formation was 52% in water with no additives as shown in Table 2, Entry 29. When basic compounds such as $NaHCO_3$ were added into the reactant solution, the selectivity for CO formation drastically increased (Entries 27, 30−34). This is due to suppressing H_2 formation under the basic condition and/or enhancement of CO_2 supply as discussed later. Similar results have been reported for a Zn-doped Ga_2O_3 photocatalyst by comparing the performances in water and an aqueous $NaHCO_3$ solution.[15] The highest selectivity reached about 90%. It indicated that the basic compound mainly affected the selectivity rather than the numbers of reacted electrons and holes. In contrast, when H_2SO_4 was added, H_2 evolution was enhanced and the CO formation was suppressed (Entry 35). NaCl and Na_2SO_4 were not effective for improving the activity for CO formation (Entries 36 and 37). We investigated to see whether the change in the selectivity of CO formation by the addition of basic compounds was due to the change in condition of the Ag cocatalyst or the role of hydrogencarbonate and/or carbonate. SEM and DRS were measured to clarify the condition of the Ag cocatalyst as shown in Figures 1 and 2. The states of the Ag cocatalysts after the reactions in water with no additives were similar to those in additions of H_2SO_4, $NaHCO_3$, Na_2CO_3 and NaOH judging from the particle size and surface plasmonic absorption of the Ag cocatalyst. These results indicated that the change in the selectivity was not mainly due to the change in the states of the Ag cocatalyst. Next, we examined the reactants for photocatalytic CO_2 reduction. In the present experiment condition in which CO formation was enhanced, because CO_2 gas is continuously bubbled, carbonate, hydrogencarbonate and solvated CO_2 molecules existed in addition of Na^+ or K^+ in the aqueous solutions. Therefore, we checked if carbonate and hydrogencarbonate ions are the reactants. Figure 3 shows photocatalytic reactions on Ag/$NaTaO_3$:Ba with not CO_2 but Ar bubbling in aqueous Na_2CO_3 and $NaHCO_3$ solutions. pH of an aqueous Na_2CO_3 solution was about 11 indicating existence of carbonate and hydrogencarbonate ions, and a negligible amount of CO_2 molecules under the equilibrium condition with Ar bubbling.[28] Only water splitting and negligible CO_2 reduction were observed under this condition. This result indicated that carbonate and hydrogencarbonate ions were not directly reduced with photogenerated electrons. On the other hand, carbonate, hydrogencarbonate ions and molecular CO_2 existed in an aqueous $NaHCO_3$ solution because the pH was about 9. CO_2 was released from the aqueous $NaHCO_3$ solution under Ar bubbling and CO simultaneously formed. The rate of CO formation decreased as the released rate of CO_2 decreased. These results indicated that the reactant was molecular CO_2 as concluded for electrochemical reduction of CO_2.[29−31]

$^{13}CO_2$ was employed to confirm the carbon source of produced CO using GC-MS with a molecular sieve-type column (Figure S1). In this isotopic experiment, $NaHCO_3$ was not added to avoid an isotopic exchange that causes mixing of $^{13}CO_2$ with $^{12}CO_2$. Only ^{13}CO was detected from $^{13}CO_2$ whereas ^{12}CO formed from $^{12}CO_2$. It was concluded from experiments using aqueous Na_2CO_3 and $NaHCO_3$ solutions and $^{13}CO_2$ that CO_2 molecules are the reactant of the photocatalytic reduction of CO_2 to form CO.

The reaction scheme of photocatalytic CO_2 reduction on Ag-cocatalyst loaded photocatalysts in water and an aqueous hydrogencarbonate solution is proposed in Figure 4.

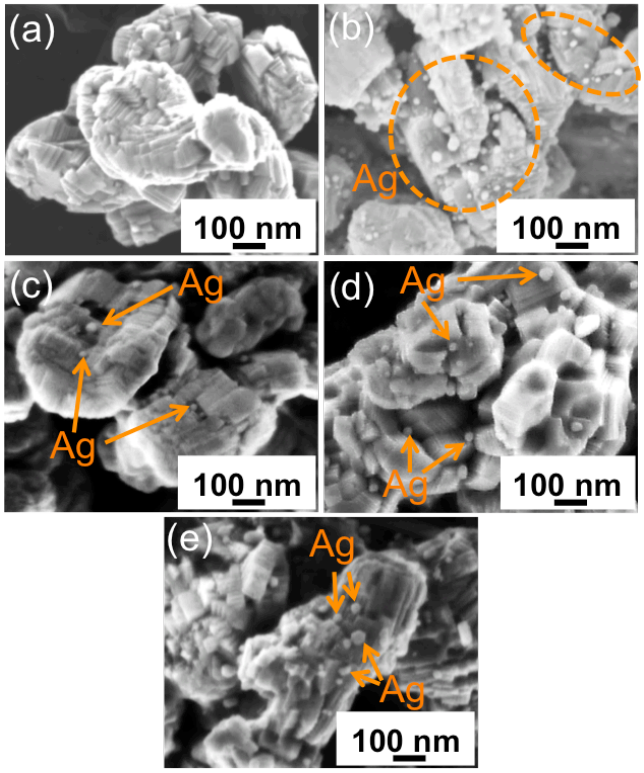

Figure 1. Scanning electron microscope images of (a) pristine $NaTaO_3$:Ba(5%), Ag(3 wt%)-loaded $NaTaO_3$:Ba(5%) after photocatalytic CO_2 reduction in (b) water and aqueous solutions containing (c) H_2SO_4, (d) $NaHCO_3$ and (e) Na_2CO_3.

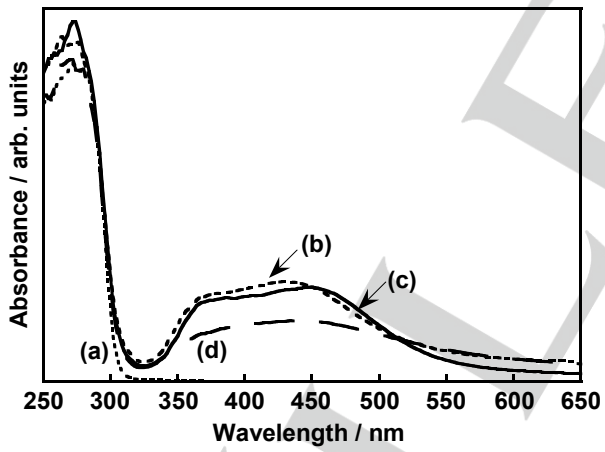

Figure 2. Diffuse reflection spectra of (a) pristine $NaTaO_3$:Ba(5%), Ag(3 wt%)/$NaTaO_3$:Ba(5%) after photocatalytic CO_2 reduction in (b) water, (c) an aqueous H_2SO_4 solution and (d) an aqueous NaOH ($NaHCO_3$) solution.

On the surface of an Ag cocatalyst;

$CO_2 + e^- \rightarrow CO_2^{\bullet-}$(ad) (1)

$H_2O + e^- \rightarrow H(ad) + OH^-$ (2)

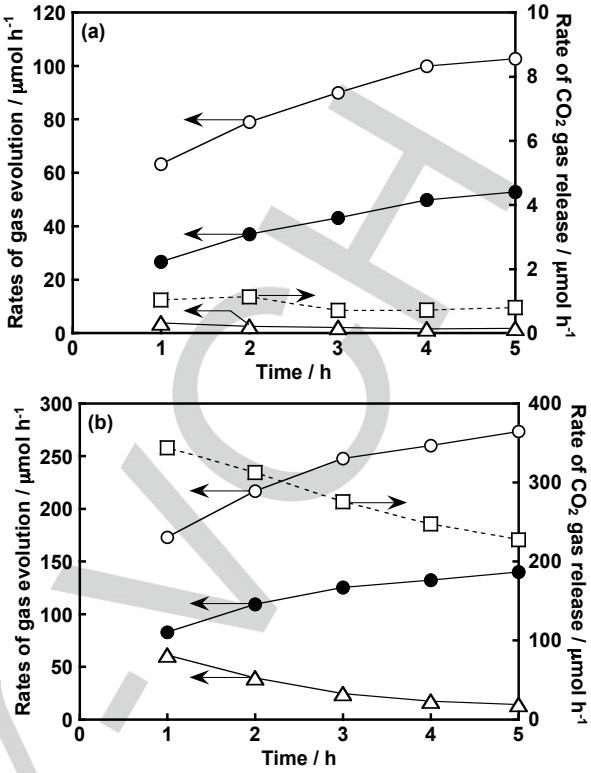

Figure 3. Reduction of CO_2 released from (a) 0.05 mol L^{-1} of an aqueous Na_2CO_3 solution and (b) 0.1 mol L^{-1} of an aqueous $NaHCO_3$ solution over Ag(3 wt%)/$NaTaO_3$:Ba(5%) photocatalyst. Photocatalyst: 0.5 g, reactant solution: 350 mL, Ar flow rate: 30 mL min^{-1}, light source: a 400 W high-pressure mercury lamp, reactor: an inner irradiation quartz cell. H_2 (○), O_2 (●), CO×10 (△) and CO_2 (□). The Ag cocatalyst was loaded by a liquid-phase reduction method.

$CO_2^{\bullet-}$ (ad) + H(ad) $\rightarrow$ CO + OH^- (3)

$2H(ad) \rightarrow H_2$ (4)

$2CO_2^{\bullet-}(ad) \rightarrow CO + CO_3^{2-}$ (5)

$CO_2^{\bullet-} + H^+ \rightarrow COOH(ad)$ (6)

$COOH(ad) + e^- \rightarrow CO + OH^-$ (7)

$CO_2 + H_2 \rightarrow CO + H_2O$ (8)

$HCO_3^- \leftrightarrow CO_2 + OH^-$ (9)

On the surface of a photocatalyst;

$2H_2O + 4h^+ \rightarrow 4H^+ + O_2$ (10)

A CO_2 molecule adsorbs on an Ag cocatalyst to form $CO_2^{\bullet-}$(ad) by capturing a photogenerated electron on the Ag cocatalyst (Eq 1). The negative charge of $CO_2^{\bullet-}$(ad) may be less than minus one. The redox potential of the $CO_2/CO_2^{\bullet-}$ couple in water is −1.9 V vs. NHE.[30] However, considering previous reports,[31] CO formation by an electrochemical reduction of CO_2 starts around −0.7 V vs. NHE at pH 0 on an Ag electrode, and the reason is considered to be the stabilization of $CO_2^{\bullet-}$ by adsorption on the Ag surface.[30] The conduction band level of a $NaTaO_3$:A (A = Mg, Ca, Sr, Ba and La) photocatalyst is about

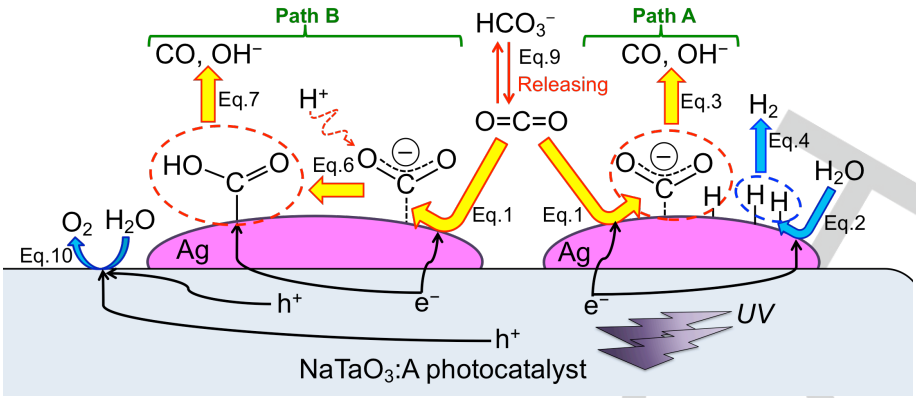

Figure 4. Proposed mechanism of CO_2 reduction to form CO over Ag-loaded $NaTaO_3$:A (A = Mg, Ca, Sr, Ba and La) photocatalysts through Path A; hydrogenation of $CO_2^{\bullet-}$(ad) and Path B; reduction of COOH(ad).

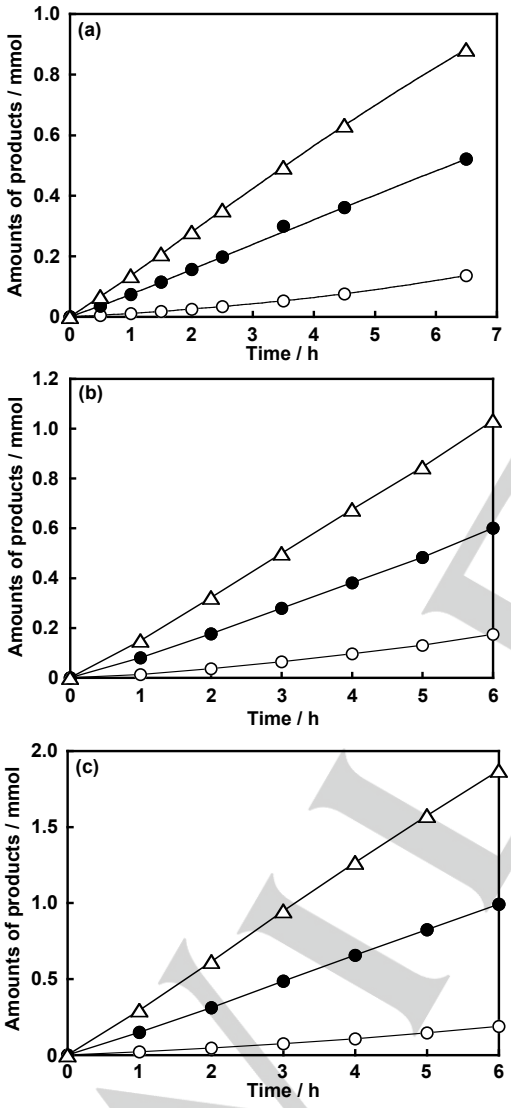

Figure 5. CO_2 reduction over (a) Ag(2 wt%)/$NaTaO_3$:Ca(5%) photocatalyst, (b) Ag(2 wt%)/$NaTaO_3$:Sr(5%) and (c) Ag(3 wt%)/$NaTaO_3$:Ba(5%) photocatalysts. Photocatalyst: 0.5−1.0 g, reactant solution: 360 mL, CO_2 flow rate: 30−100 mL min^{-1}, light source: a 400 W high-pressure mercury lamp, reactor: an inner irradiation quartz cell; H_2(○), O_2(●), CO(△).

−1.1 V vs. NHE at pH0.[20−23] Therefore, photogenerated electrons should possess the potential for the reduction of CO_2 to form $CO_2^{\bullet-}$(ad). H(ad) can be formed by the reduction of H_2O with a photogenerated electron on the Ag cocatalyst (Eq. 2). The $CO_2^{\bullet-}$(ad) species reacts with H(ad) to give CO and OH^- (Eq. 3), while a part of H(ad) is consumed to form H_2 (Eq. 4), which process is described as Path A in Figure 4. CO can also form by disproportionation of $CO_2^{\bullet-}$(ad) (Eq. 5). However, Eq. 3 is the major route to form CO rather than Eq. 5 in an aqueous solution. Another possible reaction path (Path B in Figure 4) is that H^+ attacks the $CO_2^{\bullet-}$(ad) species to form COOH(ad) (Eq. 6). The COOH(ad) species successively captures an electron to release CO and OH^- (Eq. 7). It is not excluded that some photochemical reactions of intermediates take part in the photocatalytic CO_2 reduction. Although one might think that CO_2 would react with H_2 evolved by water splitting (Eq. 8), the reaction hardly proceeds because dissociative adsorption of H_2(g) to H(ad) hardly occurs on the metallic Ag under ambient condition in an aqueous solution. The reason why the addition of a base enhances CO formation is that CO_2 molecules are smoothly supplied to the Ag surface of the reduction site of CO_2 by releasing CO_2 from hydrogencarbonate ions due to equilibrium balance (Eq. 9). In other words, hydrogencarbonate functioned as a buffer for supplying CO_2 molecules. On the other hand, O_2 forms with water oxidation by photogenerated holes on the photocatalyst surface (Eq. 10).

Figure 5 shows CO_2 reduction over the optimized Ag/$NaTaO_3$:Ca, Ag/$NaTaO_3$:Sr and Ag/$NaTaO_3$:Ba photocatalysts in an aqueous $NaHCO_3$ solution. CO and H_2 were obtained as reduction products of CO_2 and water, respectively, accompanied by O_2 evolution due to oxidation of water. The ratio of reacted electrons to holes calculated by the equation (11) was almost unity, indicating that water was an electron donor for the CO_2 reduction.

e^-/h^+ = (Sum of the number of electrons consumed for H_2 and CO formation)/(The number of holes consumed for O_2 formation) (11)

Turnover numbers of consumed electrons for CO formation to the total numbers of Ag atoms in cocatalysts on Ag/$NaTaO_3$:Ca, Ag/$NaTaO_3$:Sr and Ag/$NaTaO_3$:Ba photocatalysts calculated by

the equation (12) were 19, 22 and 13 at about 6 h of the reaction time, respectively.

$TON_{CO/Ag}$ = (The number of electrons consumed for CO formation)/(The total number of Ag atoms in a cocatalyst on a photocatalyst) (12)

The selectivities for the CO formation on Ag/$NaTaO_3$:Ca, Ag/$NaTaO_3$:Sr and Ag/$NaTaO_3$:Ba photocatalysts were 87%, 85% and 91% at about 6 h even in an aqueous medium, respectively. Thus, CO_2 reduction predominately proceeded in an aqueous medium. Ag/$NaTaO_3$:Sr and Ag/$NaTaO_3$:Ba photocatalysts (CO: 176 and 318 μmol h^{-1}; Figure 5 (b) and (c)) with 4.1 eV of the band gap showed higher activity than a Ag/$ZnGa_2O_4$ photocatalyst[16] (CO: 155 μmol h^{-1}) with 4.7 eV of the band gap under the similar experimental condition. Assuming the level of the valence band maximum of $NaTaO_3$:A (A = Sr and Ba) formed by O2p is +3.0 V vs. NHE at pH 0, the level of the conduction band minimum is −1.1 V vs. NHE at pH 0 because of 4.1 eV of the band gap.[21–23, 32] It has been reported that the conduction band minimum of $ZnGa_2O_4$ is located at more negative level than that of β-Ga_2O_3 (−1.1 V vs. NHE at pH 0).[33–35] Thus, Ag/$NaTaO_3$:A (A = Sr and Ba) photocatalysts would be thermodynamically inferior to the Ag/$ZnGa_2O_4$ photocatalyst for CO_2 reduction. However, Ag/$NaTaO_3$:A (A = Sr and Ba) actually showed higher activity than Ag/$ZnGa_2O_4$. This may be due to good affinity of an Ag cocatalyst with alkaline and La-doped $NaTaO_3$ photocatalysts that show high quantum yields for water splitting.[21–23]

Conclusions

Ag cocatalyst-loaded $NaTaO_3$:A (A = Mg, Ca, Sr, Ba and La) photocatalysts showed activity for CO_2 reduction to form CO using water as an electron donor. Among them, $NaTaO_3$:A (A = Ca, Sr and Ba) with an Ag cocatalyst loaded by a liquid-phase reduction showed the highest activity. Experiments using aqueous Na_2CO_3 and $NaHCO_3$ solutions with Ar bubbling revealed that the reactant of photocatalytic CO_2 reduction was a CO_2 molecule. Hydrogencarbonate ions functioned as a buffer to supply CO_2 molecules smoothly to the Ag cocatalyst in addition to CO_2 gas bubbling as well as suppression of H_2 formation. This resulted in the improvement of the selectivity for the CO formation up to about 90%. The synergetic effects of addition of basic compounds and CO_2 bubbling were found for photocatalytic CO_2 reduction using water as an electron donor. This effect will be able to be applied to other photocatalysts with high conduction band levels.

Experimental Section

Preparation of photocatalysts

Mg, Ca, Sr, Ba and La-doped $NaTaO_3$ powders were prepared by a solid-state reaction.[20–23] The starting materials, Na_2CO_3 (Kanto Chemical; 99.8%), Ta_2O_5 (Rare Metallic; 99.99%), MgO (Kanto Chemical; 99%), $CaCO_3$ (Kanto Chemical; 99%), $SrCO_3$ (Kanto Chemical; 99.9%), $BaCO_3$ (Kanto Chemical; 99.0%) and La_2O_3 (Kanto Chemical; 99.99%) were mixed in a mortar at the ratio of Na:A:Ta = 1.05:0.02−0.05:1. The excess amount of sodium (5 mol%) was added in the starting mixture to compensate the volatilization. The mixtures were calcined in air at 1173 K for 1 h and then 1423 K for 10 h using a platinum crucible.

Loading methods of cocatalysts

Ni, Pd, Rh, Cu, Au and Ru cocatalysts were loaded on photocatalysts by photodeposition in situ from aqueous solutions dissolving $Ni(NO_3)_2$, $PdCl_2$, $Rh(NO_3)_3$, $CuSO_4$, $HAuCl_4$ and $RuCl_3$ An NiO cocatalyst was loaded by an impregnation method. Photocatalyst powder was dispersed in an aqueous $Ni(NO_3)_2$ solution. Water of the suspension was evaporated on a water bath. The dried powder was calcined at 573 K for 1 h in air using a muffle furnace. An Ag cocatalyst was loaded by photodeposition in situ, impregnation and liquid-phase reduction methods using $AgNO_3$. In the impregnation method, the dried powder was calcined at 723 K for 1 h in air. The Ag-impregnated photocatalyst was reduced by H_2 gas at 473 K for 2 h to obtain a metallic Ag cocatalyst. In the liquid-phase reduction method, $NaPH_2O_2$ was employed as a reducing reagent. After addition of an aqueous $AgNO_3$ solution into an aqueous suspension containing the photocatalyst, an aqueous solution dissolving an equimolar amount of $NaPH_2O_2$ to Ag^+ was added into the suspension. The mixture was stirred at 333 K for 1 h. The obtained Ag-loaded photocatalysts were washed with water and were collected by filtration.

Characterization of photocatalysts

The photocatalysts obtained were identified by powder X-ray diffraction (Rigaku; Miniflex, Cu Kα). Diffuse reflection spectra were recorded on a UV-vis-NIR spectrometer (JASCO; UbestV-570) and were converted from reflection to absorbance by the Kubelka-Munk method. Photocatalysts and cocatalysts loaded were observed using a scanning electron microscope (JEOL; JSM-6700F).

Photocatalytic reactions

Photocatalytic reactions were carried out using a gas-flow system with an inner irradiation cell made of quartz equipped with a 400 W high-pressure mercury lamp as a light source. Photocatalyst powder (0.25–1.0 g) was dispersed in water (350–370 mL). CO_2 gas was bubbled into the suspension at about 30−100 mL min^{-1} of a flow rate. H_2SO_4 (Kanto Chemical; 96.0%) NaCl (Kanto Chemical; 99.5%), Na_2SO_4 (SIGMA-ALDRICH; 98%), $NaHCO_3$ (Wako Pure Chemical; 99.5%), $KHCO_3$ (Wako Pure Chemical; 99.5%), Na_2CO_3 (Kanto Chemical; 99.8%), K_2CO_3 (Kanto Chemical; 99.5%), NaOH (Kanto Chemical; 95.0%) and KOH (Kanto Chemical; 86.0%) were added into the reactant solution, if necessary. Gas products of H_2, O_2, CO and CH_4 were determined using gas chromatographs (Shimadzu; GC-8A) with a thermal conductivity detector (MS-5A, Ar carrier) and a flame ionization detector (MS-13X, N_2 carrier) with a methanizer. An aqueous product of formic acid was analyzed

using an ion chromatograph (TOSOH; IC-2010, TSKgel SuperIC-Anion HS).

Isotope experiment

$^{13}CO_2$ gas (SIGMA-ALDRICH; 99.5 atom%) was employed for an isotope experiment to confirm the carbon source of CO formed by photocatalytic CO_2 reduction. The products were detected using a GC-MS (Shimadzu; GCMS-QP2010 Plus, RESTEK; RT-Msieve 5A).

Acknowledgements

This work was supported by Grants-in-Aid (No. 24246131) for Scientific Research and the ENEOS hydrogen foundation.

Keywords: Carbon dioxide fixation • Energy conversion • Photocatalysis

[1] S. C. Roy, O. K. Varghese, M. Paulose, C. A. Grimes, *ACS Nano*, **2010**, *4*, 1259-1278.
[2] S. N. Habisreutinger, L. Schmidt-Mende, J. K. Stolarczyk, *Angew. Chem. Int. Ed.*, **2013**, *52*, 7372-7408.
[3] M. Tahir, N. S. Amin, *Energy Convers. Manage.*, **2013**, *76*, 194-214.
[4] J. Mao, K. Li, T. Peng, *Catal. Sci. Technol.*, **2013**, *3*, 2481-2498.
[5] J. L. White, M. F. Baruch, J. E. Pander III, Y. Hu, I. C. Fortmeyer, J. E. Park, T. Zhang, K. Liao, J Gu, Y. Yan, T. W. Shaw, E. Abelev, A. B. Bocarsly, *Chem. Rev.*, **2015**, *115*, 12888-12935.
[6] K. Sayama, H. Arakawa, *J. Photochem. Photobiol. A: Chem.*, **1994**, *77*, 243-247.
[7] K. Sayama, H. Arakawa, *J. Phys. Chem.*, **1993**, *97*, 531-533.
[8] Y. Miseki, H. Kato, A. Kudo, *Energy Environ. Sci.*, **2009**, *2*, 306-314.
[9] K. Iizuka, T. Wato, Y. Miseki, K. Saito, A. Kudo, *J. Am. Chem. Soc.*, **2011**, *133*, 20863-20868.
[10] Y. Negishi, M. Mizuno, M. Hirayama, M. Omatoi, T. Takayama, A. Iwase, A. Kudo, *Nanoscale*, **2013**, *5*, 7188-7192.
[11] T. Takayama, K. Tanabe, K. Saito, A. Iwase, A Kudo, *Phys. Chem. Chem. Phys.*, **2014**, *16*, 24417-24422.
[12] T. Takayama, A. Iwase, A. Kudo, *Bull. Chem. Soc. Jpn.*, **2015**, *88*, 538-543.
[13] S. Iguchi, K. Teramura, S. Hosokawa, T. Tanaka, *Catal. Sci. Technol.*, **2016**, *6*, 4978-4985.
[14] K. Teramura, H. Tatsumi, Z. Wang, S. Hosokawa, T. Tanaka, *Bull. Chem. Soc. Jpn.*, **2015**, *88*, 431-437.
[15] K. Teramura, Z. Wang, S. Hosokawa, Y. Sakata, T. Tanaka, *Chem. Eur. J.*, **2014**, *20*, 9906-9909.
[16] Z. Wang, K. Teramura, S. Hosokawa, T. Tanaka, *J. Mater. Chem. A*, **2015**, *3*, 11313-11319.
[17] Z. Wang, K. Teramura, S. Hosokawa, T. Tanaka, *Appl. Catal. B: Environ.*, **2015**, *163*, 241-247.
[18] H. Yoshida, L. Zhang, M. Sato, T. Morikawa, T. Kajino, T. Sekito, S. Matsumoto, H. Hirata, *Catal. Today*, **2015**, *251*, 132-139.
[19] A. Iwase, S. Yoshino, T. Takayama, Y. H. Ng, R. Amal, A. Kudo, *J. Am. Chem. Soc.*, **2016**, *138*, 10260-10264.
[20] A. Kudo, H. Kato, *Chem. Phys. Lett.*, **2000**, *331*, 373-377.
[21] H. Kato, K. Asakura, A. Kudo, *J. Am. Chem. Soc.*, **2003**, *125*, 3082-3089.
[22] A. Iwase, H. Kato, H. Okutomi, A. Kudo, *Chem. Lett.*, **2004**, *33*, 1260-1261.
[23] A. Iwase, H. Kato, A. Kudo, *ChemSusChem*, **2009**, *2*, 873-877.
[24] M. Li, Peng Li, K. Chang, T. Wang, L. Liu, Q. Kang, S. Ouyang, J. Ye, *Chem. Commun.*, **2015**, *51*, 7645-7648.
[25] V. Jeyalakshmi, R. Mahalakshmy, K. R. Krishnamurthy, B. Viswanathan, *Catal. Today*, **2016**, *266*, 160-167.
[26] F. Fresno, P. Jana, P. Reñones, J. M. Coronado, D. P. Serranob, V. A. de la Peña O'Shea, *Photochem. Photobiol. Sci.*, **2016**, DOI: 10.1039/c6pp00235h
[27] A. Iwase. H, Kato, A. Kudo, *Appl. Catal. B: Environ.*, **2013**, *136-137*, 89-93.
[28] H. Zhong, K. Fujii, Y. Nakano, F. Jin, *J. Phys. Chem. C*, **2015**, *119*, 55-61.
[29] Y. Hori, K. Kikuchi, S. Suzuki, *Chem. Lett.*, **1985**, 1695-1698.
[30] Y. Hori, H. Wakebe, T. Tsukamoto, O. Koga, *Electrochim. Acta*, **1994**, *39*, 1833-1839.
[31] T. Hatsukade, K. P. Kuhl, E. R. Cave, D. N Abram, T. F. Jaramillo, *Phys. Chem. Chem. Phys.*, **2014**, *16*, 13814-13819.
[32] A. Kudo, Y. Miseki, *Chem. Soc. Rev.*, **2009**, *38*, 253-278.
[33] X. Wang, Q. Xu, M. Li, S. Shen, X. Wang, Y. Wang, Z. Feng, J. Shi, H. Han, C. Li, *Angew. Chem. Int. Ed.*, **2012**, *51*, 13089-13092.
[34] X. Wang, S. Shen, S. Jin, J. Yang, M. Li, X. Wang, H. Han, C. Li, *Phys. Chem. Chem. Phys.*, **2013**, *15*, 19380-19386.
[35] Z. Wang, K. Teramura, Z. Huang, S. Hosokawa, Y. Sakata, T. Tanaka, *Catal. Sci. Technol.*, **2016**, *6*, 1025-1032.

10.1002/cssc.201601360

WILEY-VCH

Entry for the Table of Contents

FULL PAPER

Text for Table of Contents

Loading of an Ag cocatalyst and addition of bases realize highly active and selective CO_2 reduction to form CO using water as an electron source over $NaTaO_3$:A (A = Mg, Ca, Sr, Ba and La) photocatalysts.

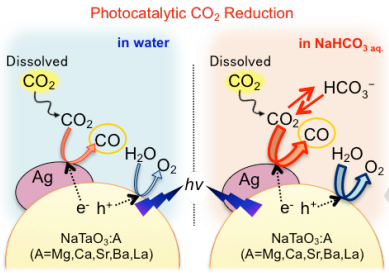

*Haruka Nakanishi, Kosuke Iizuka, Tomoaki Takayama, Akihide Iwase, Akihiko Kudo**

Page No.1 – Page No.7

Highly Active Alkaline Earth Metals and Lanthanum-Doped $NaTaO_3$ Photocatalysts for CO_2 Reduction to Form CO Using Water as an Electron Donor